

Balloon Animal Robots: Reconfigurable Isoperimetric Inflated Soft Robots

Anthony D. Stuart, Zachary M. Hammond, Sean Follmer

I. ABSTRACT

This paper introduces a new class of soft reconfigurable robot: balloon animal robots. The balloon animal robot consists of a closed volume inflatable tube which can be reconfigured into structures of varying topology by a collective of simple sub-unit robots. The robotic sub-units can (1) drive along the length of the tube to localize a joint, (2) create pinch points that locally reduce the bending stiffness of the tube to form a joint, and (3) selectively mechanically couple to one another through cable driven actuators to create nodes of the structure. In this work we introduce the hardware necessary to construct the robot, present experiments to guide the hardware design, and formulate an algorithm using graph theory to calculate the number of nodes and node connections needed to form different 2D shapes. Finally, we demonstrate the system with two active nodes and four passive nodes forming multiple 2D shapes from the same hardware.

II. INTRODUCTION

A. Overview

As robots move from highly-engineered environments into the outside world, there is a growing need to design robots that are robust, safe, and capable of navigating varied terrain. Since engineers often cannot predict exactly what type of obstacles or environments their robot will have to navigate through, robots with the ability to change their shape to fit the desired scenario can allow for the completion of more varied and complex tasks [1]. The goal of this research is to develop a reconfigurable robot that is capable of large global morphology and topology change while also being sturdy and safe around humans. One physical example of a soft object capable of dramatic shape change is a balloon animal. Through the process of twisting a single straight balloon at various points to define joints and bending the balloon at these defined locations, structures ranging from rigid trusses with load-bearing capabilities to dog-shaped quadrupeds can be formed [2].

Taking inspiration from balloon twisting, we propose a new class of reconfigurable soft robot based on this concept. The robot is able to create a number of pinch points on a single tube to form segments of arbitrary length and bring the pinch points together to fold the tube into complex structures. To accomplish this, the robot consists of a closed-volume inflatable tube and a collective of simple sub-unit robots

The authors are with the Dept. of Mechanical Engineering, Stanford University, Stanford, CA 94304, USA adstuart@stanford.edu. This work is supported in part by the National Science Foundation Award # 1925030.

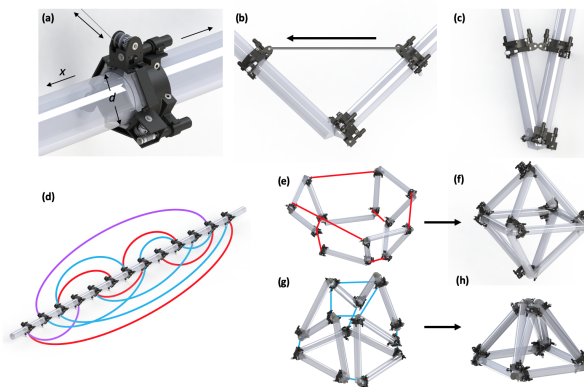


Fig. 1. (a) The robot is composed of a number of sub-unit node robots that are interconnected by strings. Each robot can drive along the length of an inflated tube, cinch the tube to create effective joints, and change the length of their string connection. (b) two of the three node robots shown here are connected by a string, while the third creates an effective joint between them. (c) When this string is shortened, the two node robots are brought together, structural nodes are merged together to form a single node. (d) A robot layout capable of re-configuring to the structures shown in (f) and (h). Red strings are engaged to make the shape in (f), blue strings are used to make the shape in (h), and purple strings are used to make both. (e) and (g) show intermediate steps for forming two different shapes, while (f) and (h) show the respective completed shapes

(Fig. 1(a)). Each sub-unit robot is capable of driving along the tube to localize joints, creating cinch points to locally reduce bending system and create joint, and pulling itself towards other robots using predetermined string connections as shown in Fig. 1(a-c). At design-time, several goal topologies consisting of distinct shapes are selected. We then use these topologies to determine the robot layout consisting of the number of sub-unit node robots and the string connections between them (Fig. 1(d)). During operation, the system can switch between the goal topologies by selectively pulling and releasing the string connections between the node robots (Fig. 1(e-h)). In addition, the geometry can be changed by modifying the link lengths - allowing for both topological and geometric changes. However, this change is constrained by the total length of the tube, making it an isoperimetric robot [3].

Balloon animal robots have a number of advantages. They can reconfigure into a wide variety of different shapes to better suit different tasks. Examples of this could potentially include a quadruped mode for locomotion, a snake mode for navigating through tight spaces, and a truss mode for withstanding heavy loading as shown in Fig. 1(f) and Fig. 1(h). The inflated tubes that make up this class of robot provide a sturdy construction while also being soft and

capable of deforming under loading. This is demonstrated by the robot from [3], which can withstand forces over 350 N. Force deflection and buckling behavior of inflated beams has been modeled in previous work [4], [5]. The individual node robots are also simple and identical, allowing for easy manufacturing and repair.

In this paper we present the mechanical design of the system in Section III, experiments to measure relevant forces in Section IV, the algorithm developed to generate a robot layout in Section V, and a 2D demonstration of the system morphing into different shapes in Section VI.

B. Related work

This research builds on the work done in the areas of reconfigurable robots, soft robots, tensegrity robots, and truss robots.

1) *Modular Reconfigurable Robots:* Reconfigurable robots are made up of multiple identical small modules that are able to change their position in relation to each other, resulting in an overall morphology and topology change [6]. The fact that reconfigurable robots are made up of repeated sub-units gives them the potential to be highly adaptable while also consisting of easy to mass produce and replace components [7]. Within the field of reconfigurable robots, prior research has explored wheeled-modules that manipulate passive structural frames to enable coordinated transportation of objects [8], [9]. Our balloon animal robot shares similarities to this class of robot as it consists of multiple repeated node robots attached to a passive structure. However, an importance difference is that our modules are manipulating a passive structure to form the global topology rather than using the structure primarily as a means to couple sub-robots together. The actions of the modules are mediated by this passive structure, enabling complex behaviors at the system level while reducing complexity at the module level.

2) *Soft Robots:* Soft robots are made out of highly compliant materials, allowing them to easily deform under external loads [10]. This compliance grants these systems an inherent adaptability and safety, making them desirable for navigating complex environments or operating around humans [11]. Prior work has been done in this field involving thin-walled inflated tubes, both as the primary structure for robots [12], [13] as well as the basis of soft actuators driven by pressure differentials [14], [15]. Our system's structure also revolves around an inflated tube, but differs from these examples in that it uses tension members rather than pressure differences to actuate, allowing for operation without an on-board pump and the potential for more energy efficient reconfiguration. Other relevant work within the field of soft robotics involves reducing local stiffness to create joints. Prior research has accomplished this by designing creases into the material [16], utilizing layer jamming [17], inflating a soft bladder [18], applying negative pressure [19], and pinching the tube with rollers [3]. Our node robots use a similar joint creation method as [3] by cinching the tube to decrease stiffness, but our ability to both add and remove these joints as well

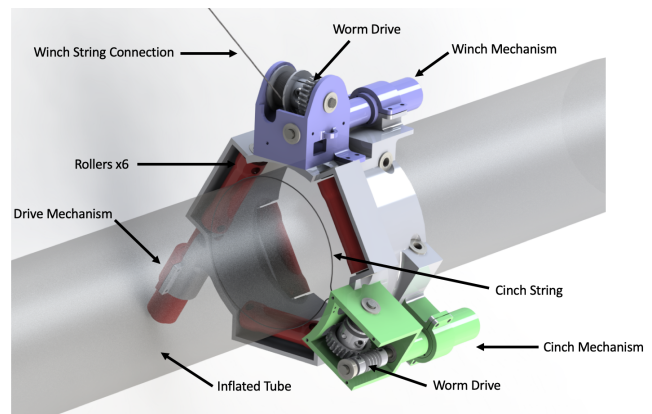


Fig. 2. 3D model of a node robot with the three key subsystems highlighted. The cinch mechanism is shown in green, the winch mechanism is shown in blue, and the drive mechanism is shown in red.

as bring them together during operation allows for greater potential topology and morphology change.

3) *Tensegrity Robots:* Tensegrity robots are made up of disconnected compression members connected by tension members in a stable network [20]. By manipulating the length of these members, tensegrity robots are capable of locomotion and shape change [21]. The tension members that support the robot are also compliant, making them capable of withstanding large impacts and traversing rough terrain [22], [23]. Our system shares some similarities with tensegrity robots. It also consists of a structure of compression and tension members in the form of inflated tube segments and string connections, and it uses actuated cables to deform the system's structure to enable actuation. However, our robot's ability to change both the length and overall number of the compressive segments in the system by localizing and creating joints enables greater overall shape change.

4) *Truss Robots:* The field of truss robotics consists of robots that take the form of truss-like structures with members that can grow and shrink in length (usually through the use of linear actuators) allowing for overall shape change [24]–[30]. These robots benefit from the structural efficiency of trusses, while also having the flexibility of changing shape. Within the field of truss robotics, there has also been some work on soft trusses, which change shape by driving nodes along a tube [3]. Our robot shares many similarities to this soft truss robot. However, rather than having a fixed overall truss structure limited to changing the length of individual members, our system is free to reconfigure into a much wider variety of shapes, drawing inspiration from Variable Topology Trusses [29].

III. MECHANICAL DESIGN

The balloon animal robots consist of two key elements: a thin-walled inflated tube and a set of n node robots that (1) localize by driving along the tube, (2) create joints using a cinch mechanism, and (3) actuate these joints to form goal topologies. In this section we discuss these three main functions of the node robots.

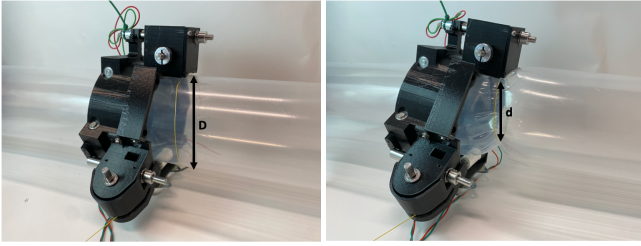


Fig. 3. The cinch mechanism in its uncinched (*left*) and cinched (*right*) state. D refers to the original diameter of the tube, while d refers to the cinched diameter

A. Localizing Joint: Driving Along the Tube

The node robots are capable of driving along the tube to re-position themselves with respect to each other. Two stacks of three rollers arranged in alternating triangles contact the tube as shown in red in Fig. 2. This configuration and number of rollers is used to prevent the robot from rotating perpendicular to the tube’s axis and to evenly distribute reaction forces on the tube. One of these six rollers is powered by a motor (Pololu #3046) and covered in silicone to provide a high-friction contact with the tube, while the others are passive. The motor is currently driven open loop, but future work will involve incorporating closed loop control for more accurate positioning. The rollers as well as the node’s overall frame is 3D printed using PLA filament. The node’s ability to drive along the tube allows for the robot to change the lengths of the members of the final structure, enabling morphological change. It also enables the robot to move the location that string edges exert forces on the robot, allowing the tube to bend and actuate in specific directions.

B. Creating Joints: Cinching the Tube

Effective joints can be created in thin-walled inflated tubes by creating localized regions of low-bending stiffness ([3], [16], [17]). We accomplish this with a cinching mechanism consisting of a loop of string connected to a motorized winch on one end and a fixed point of the robot frame on the other (shown in green in Fig. 2). As the winch pulls the string, the diameter of the loop decreases, squeezing the tube and predisposing it to bend at the location of the cinch. (Fig. 3). The winch is driven by a motor (Pololu #3046) coupled to a non-backdrivable worm gear, allowing the mechanism to maintain its cinch without expending energy. The ability of the node robots to create and remove joints by cinching and releasing the tube allows us to change the number of nodes in our structures, enabling a wide range of morphological and topological change. This also allows us to vary the stiffness (and thus stored energy when bent) in each joint by changing the cinch diameter.

C. Actuating Joints: Forming Goal Topologies

Once a joint has been created, nodes are brought together using a winch and cable system, as seen in blue in Fig. 2. Each node contains a motorized spool of fishing line, as well as a fixed mounting point that another node’s string can

be tied on to. When the winch is activated, the two nodes are pulled together (Fig. 1(b)). Doing this will result in the tube bending around the point of lowest stiffness, which can be determined by creating a cinch somewhere between the two nodes with another node robot. This process of bringing nodes together allows us to alter the structural topology of our robot. Similar to the cinch mechanism, this subsystem is powered by a motor (Pololu #3046) attached to a worm drive, allowing for the tube to remain in its bent state without any holding torque from the motor. In this work we demonstrate node robots with one winch. However, more winches can also be added to a node robot to increase connectivity.

IV. EXPERIMENTS

To better understand how cinching the tube impacts the force needed to bend around the created joint, we conducted experiments using the same experimental setup. The setup comprised of a 34.5 kPa pressurized tube of 10.16 cm diameter fixed to a table, a digital protractor secured along the tube, a force sensor, and a 0.46 cm wide nylon zip-tie with markings in 2.54 cm increments. The pressurized tube consisted of a fabric outer tube made of 200-denier nylon and a low-density polyethylene inner tube. The zip-tie was placed at a known location on the tube and cinched to a desired diameter, while the force sensor was pulled perpendicular to the tube until the desired joint bend angle was reached.

The first relationship we investigated was between cinching diameter and the torque required to bend the tube. As seen in Figure 4, we selected three cinch diameters (8.5 cm, 6.9 cm and 3.7 cm) and measured the torque required to bend the tube across a range of angles from 10 to 135 degrees. At low bend angles, reducing the cinch diameter resulted in a significant reduction in joint torque. At the smallest angle of 10 degrees, reducing the cinch diameter from the largest diameter of 8.5 cm to the smallest one of 3.7 cm resulted in a 93% reduction in joint torque from 6.2 Nm to 0.4 Nm. The effect of this reduction in diameter appears to decrease gradually until a critical angle after which the difference between the bending torques are negligible. This critical angle coincides with angles at which we observed the material of the tube interfering with itself. This suggests that at large angles, the interference between the tube is the dominant contributor to the joint torque. Cinching the tube to smaller diameters delays the angle at which the two sides of the tube come in contact, resulting in lower joint torques at small angles.

The second relationship we investigated was the amount of force needed to cinch the tube to different diameters. This was done by pulling on the zip-tie wrapped around the tube to an indicated displacement and measuring the required force with a force sensor. We evaluated six pull distances from 2.54 to 15.24 cm. As seen in Fig. 5, we found that the cinching force increases roughly linearly the greater the diameter is reduced, going from around 100 N at 2.54 cm of diameter reduction to around 240 N at 15.24 cm. As the cinch diameter is reduced, the applied energy is stored or lost through a number of modalities. As the membrane of an inflated

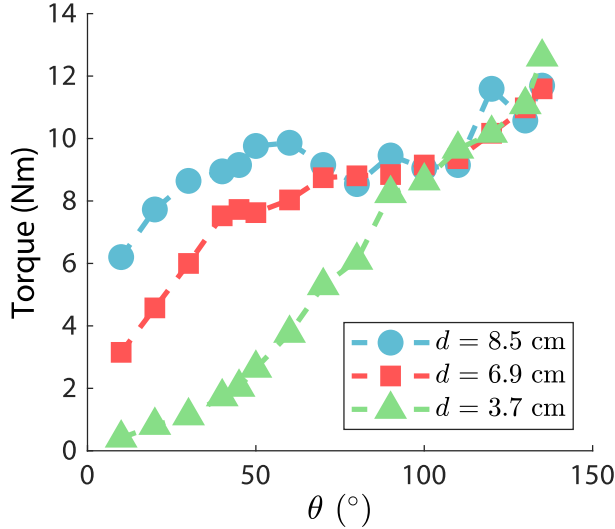


Fig. 4. Torque needed to bend a 34.5 kPa pressurized tube of uncinched diameter D to a specific angle θ for three different cinched diameters d

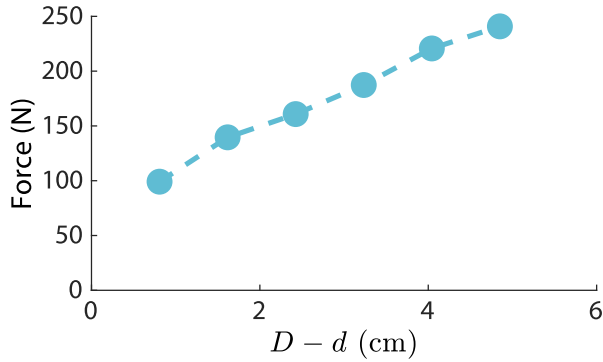


Fig. 5. Force required to cinch a the tube from its starting diameter D to a new diameter d

structure is deformed, work is done in stretching the tube membrane, bending the tube membrane, and compressing the gas [31]. There are also frictional losses due to the relative motion between surfaces in contact including the zip-tie and the tube (a capstan-like effect), the two layers of the tube membrane (a layer-jamming-like effect), and within the zip-tie itself.

Considering the data shown in Fig. 4 and Fig. 5 we can estimate the requisite energy necessary to create a cinch of a specified diameter and bend the tube to a desired angle. Creating a small diameter cinch requires a large upfront energetic cost, which is, ideally, compensated for in lower joint stiffness. However, if the desired angle is small, we may spend more energy creating the joint than we save in lower stiffness. To understand this trade-off, we compute total energy to create the joint and bend the tube to a desired angle. The energy required to make a cinch of a given diameter is the area under the curve in Fig. 5 scaled by π (we use a linear fit of the experimental data). The energy

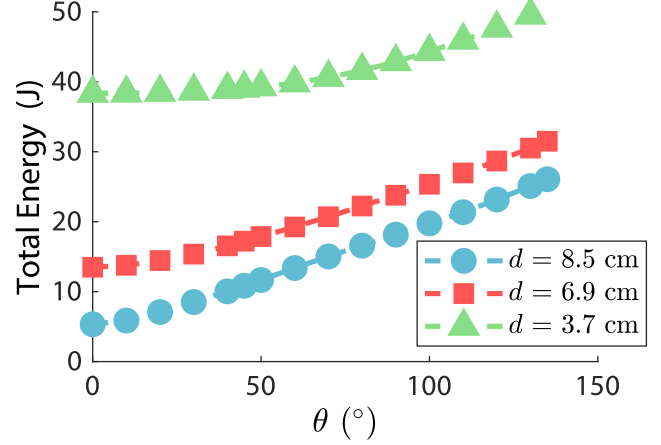


Fig. 6. Total energy to create a cinch of a specific diameter, d , and bend the tube to angle θ .

required to bend the tube to a given angle, θ , is the area under the curve in Fig. 4 (where all curves are assumed to include the origin). The results are shown in Fig. 6. We find that the energy to create the cinch is much higher than the potential energy savings due to reduced stiffness which is evident by the fact that the curves in Fig. 6 do not intersect. It is necessary to create at least a large diameter cinch so that we can localize the joint as in [17], however, creating a small diameter cinch is energetically expensive. If, instead of creating a passive structure, we were creating a joint that would be bent repeatedly over time, then the energy savings due to a small diameter cinch would accumulate.

V. GENERATING SHAPE CONFIGURATIONS

In this section we will discuss algorithms we developed to generate the requisite robot layouts to assume the physical forms described by the goal topologies. To do this, it is useful to mathematically describe the robot as an undirected graph, as previously shown in work analyzing the construction of polyhedra with balloons [2] and work in truss robotics [32], [33]. In [2], the balloon (or tube) is represented as edges in a graph, and the twists (or cinches) in the balloon are represented as nodes. In our work, we also must represent the strings that connect node robots together. Therefore, we describe two sets of edges: tube edges that represent the segments of the tube, and string edges that describe the string connections between node robots. Formally, the graph describing the robot is denoted as a set of n nodes, m tube edges, and p string edges: $G = \{V, \mathcal{E}_t, \mathcal{E}_s\}$, where $V = \{1, \dots, n\}$ is the set of nodes of the graph, $\mathcal{E}_t = \{\dots, \{i, j\}, \dots\}$ is the set of undirected tube edges ($|\mathcal{E}_t| = m$), and $\mathcal{E}_s = \{\dots, \{i, j\}, \dots\}$ is the set of undirected string edges ($|\mathcal{E}_s| = p$).

Our primary concern is developing the robot layout that provides the means to reconfigure to the different goal topologies and must be determined at design-time. For simplicity and clarity, we ignore the lengths of the edges, which can be altered during run-time. For our robot, run-time is

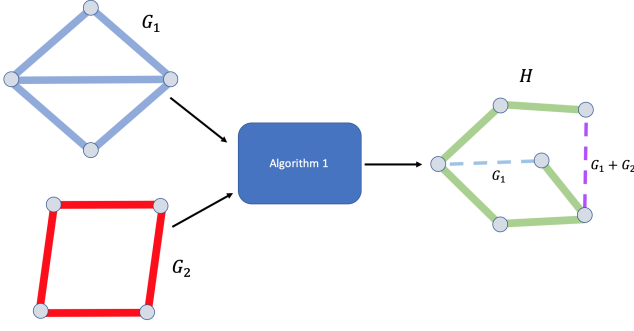


Fig. 7. Visual representation of Algorithm 1. A set of graphs representing desired structures are input (*left*), and a graph showing the optimal location of node robots and string attachments necessary to form the structures is output (*right*).

when the N shapes can be configured by a combination of cinching and pinching. Our algorithm does not determine run-time control inputs to effect reconfiguration, which has been explored in other contexts [33], [34].

Determining the robot layout amounts to computing the necessary number of node robots and the string edges that interconnect them. Given a set of goal topologies, the corresponding robot layout is not unique. Therefore, we attempt to find a robot layout that minimizes the number of string edges, reducing the mechanical complexity of the robot. To find the optimal robot layout, we developed an algorithm that we describe in two parts. Algorithm 1, is the high level optimization that determines the robot layout with the fewest string edges. Algorithm 2, which is repeatedly called by Algorithm 1, is a helper function that generates candidate robot layouts to be considered by Algorithm 1. A visualization of this process is shown in Fig. 7. The graphs, G_1 and G_2 , on the left hand side are goal topologies that are passed into the algorithm which returns the robot layout, H .

A. Finding Optimal Robot Layout

Algorithm 1 takes a set of graphs, each representing a desired goal topology, as an input and returns a graph representing the robot layout containing the fewest string edges. The algorithm starts by checking that each of the input graphs contains a valid Eulerian path. Graphs that do not have an Eulerian path cannot be constructed physically from a single continuous tube [2]. Physical structures that do not have an Eulerian path can be modified with redundant edges so that they have an Eulerian path [2]. We take the assumption that our goal topologies will have Eulerian paths.

The algorithm generates every possible Eulerian path for each goal topology. The length of the longest Eulerian path corresponds to the number, n , of node robots our robot layout will have. The elements of a path correspond to the nodes of the goal topology. The indices of this path correspond to the nodes of the robot layout. Indices that share the same element correspond to node robots that are connected by string edges. Eulerian paths that are shorter than n do not require use of every node robot in the robot layout. Therefore, one or

Algorithm 1: Find Optimal Robot Layout

Input: Set of desired graph structures G containing graphs $G_1 : G_n$
Output: Optimal graph of single tube w/ string connection: H_{best}
if all graphs in G contain Eulerian paths **then**
 Generate sets of all modified Eulerian paths for $G_1 : G_n \rightarrow p_1 : p_n$;
 for each P that is a possible combo of $p_1 : p_n$ **do**
 $H = \text{Create Robot Layout}(P)$;
 Count number of string edges in H ;
 if current # string edges < previous best **then**
 $H_{best} = H$;
 Update the previous best value ;
 end
 end
end
return H_{best} ;

more node robots will be disengaged and will not form a cinch. The algorithm generates modified Eulerian paths for paths with less than n elements that indicate which node robots will be disengaged. The modified Eulerian paths are created from copies of the Eulerian paths that are altered through the insertion of an identifier at indices corresponding to disengaged node robots. A new modified Eulerian path is created for every possible combination of disengaged node robots for each Eulerian path.

Once all the modified Eulerian paths are generated, the algorithm selects one path for each graph and places it into a set, which is passed into Algorithm 2. Algorithm 2, described in further detail below, takes this set and returns a candidate robot layout describing its physical construction with node robots and string edges. Algorithm 1 then counts the number of string edges in this robot layout. If the candidate robot layout has less strings than previous candidates, it is saved as the current best robot layout. This process is repeated for every possible set of modified Eulerian paths, ensuring, through brute force, that the final robot layout is the optimal solution. While we chose to optimize for the lowest number of active nodes and strings in this paper, other goals such as maximizing the number of potential shapes could also be considered in future work. An example of the algorithm's inputs and output can be seen in Fig. 8.

B. Creating Robot Layout

Algorithm 2 takes a set of modified Eulerian paths as an input, and returns the respective robot layout capable of forming every goal topology. The algorithm starts by determining the length of the modified Eulerian paths, n , and initializing a graph with n nodes and tube edges that connect them in series. The algorithm searches the input paths and adds new string edges to the robot layout when it finds nodes that must be connected.

In the case of a single input path, any nodes that appear

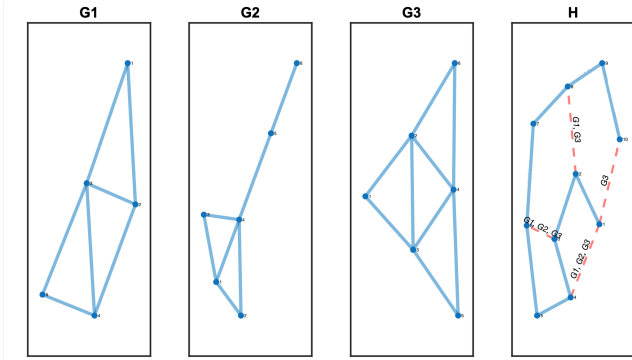


Fig. 8. G1, G2, and G3 are the input goal topologies to Algorithm 1, while H is the output optimal robot layout. Tube edges are indicated by solid blue lines, while string edges are shown as dashed red lines. The labels on the string edges correspond to the input goal topology formed by fully winching the connected nodes together.

only once are unmodified in the new graph. Nodes that appear t times are represented in the new graph as a group of t nodes connected by $t - 1$ string edges. All of the nodes in the new graph have two tube edges, with the exception of the end nodes which have one. The resulting graph is a straight tube with the same number of tube edges as the original graph, but with additional nodes equal to the number of added string edges.

In the case of multiple input paths, the process of adding string edges is repeated, using the output graph from the previous iteration as a starting point. Before adding a new string edge between two nodes, the algorithm checks to see if one already exists between those nodes. If one does, the algorithm indicates the existing edge is used by both paths.

VI. DEMONSTRATION

We demonstrate the shape-changing capabilities of this robot by creating multiple 2D structures using the same setup of node robots and string connections. We select four graph structures as goal topologies, as seen on the right side of Fig. 9, from which we generate the robot layout showing the required number of node robots and inter-node connections necessary to form the shapes. In this case, our design requires a total of seven node robots and three string connections. For the purposes of the demonstration, two of the three node robots attached to cables are actuated, while the remaining passive joints are created using zip-ties. A zip-tie is also used in place of one of the three string connections determined by the robot layout to connect the two ends of the tube together and form a loop. While zip-ties were used to simplify manufacturing for the demonstration, in practice actuated joints and string connections would be used for all nodes. To start the demonstration, a low-density polyethylene tube measuring 10.16 cm in diameter is inflated to 34.5 kPa, and the active node robots are placed into one corner as seen in Fig. 9(a). To form the shape in Fig. 9(b), both node robots drive to the center of their respective tubes, after which the left node robot cinches to create a joint and activates its winch to fully pull itself towards its passive node. To form

Algorithm 2: Create Robot Layout

Input: Set of modified Eulerian paths : P
Output: Graph of robot layout: H
 $n = \text{length of paths in } P$;
 Create graph H with n nodes;
 $\mathcal{E}_t(H) = \{\{1, 2\}, \{2, 3\}, \dots, \{n-1, n\}\}$;
for each path $\in P$ **do**
 Initialize an empty map, $visitedNodes = \{\}$;
 for $i = 1:n$ **do**
 $node = path[i]$;
 if $node = 0$ **then**
 Do nothing;
 else if $node \in visitedNodes$ **then**
 $k = visitedNodes[node]$;
 if $\{i, k\} \notin \mathcal{E}_s(H)$ **then**
 Add $\{node, k\}$ to $\mathcal{E}_s(H)$
 end
 else
 $visitedNodes[node] = i$;
 end
 end
end
return H ;

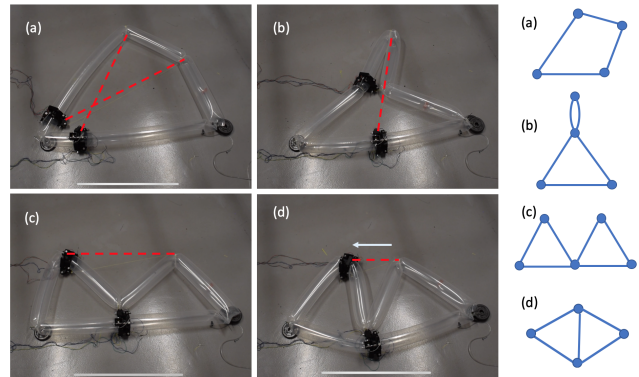


Fig. 9. A demonstration of the robot forming four different goal topologies shown at the right. The red dashed lines indicate string connections between node robots.

the shape in Fig. 9(c), the left node robot releases tension from its winch while the bottom node robot's winch pulls its associated passive node towards itself. The final shape in Fig. 9(d) is then formed by the bottom node robot cinching to create a joint and the left node robot once again activating its winch to fully pulling itself towards its passive node.

VII. CONCLUSION

This paper introduced a new type of reconfigurable soft robot inspired by balloon animals, which uses node robots to manipulate a thin-walled inflated tube into different topologies. Design of the mechanical system and an algorithm used to generate robot layouts was described, and the robot's ability to form 2D goal topologies was demonstrated.

While the current demonstration of this robot is limited to forming static 2D structures, additional node robots could be constructed to demonstrate more complex 3D shapes. Additional work could also be done designing a system to automatically attach and detach string connections between nodes. This would allow for more reconfigurability and would require less advanced shape planning by the robot operator. The mechanical design of both the node robots and the tube itself can also be improved. In future versions of the node robot, we plan to include encoders and a micro-controller to enable closed-loop control of all of the robot's degrees of freedom. We also plan to experiment with a more wear-resistant tube design that is more robust to repeated cinching than our current prototype.

Future work could also include modifying our algorithm to generate robot layouts that contain actuated segments where additional tension members are used to control free degrees of freedom rather than passive structures. Another future direction could be to develop a new algorithm to generate step-by-step instructions to move from one goal topology to another rather than simply generating an overall layout. We could also explore different optimization goals such as maximizing the number of potential shapes that a given robot layout can form.

REFERENCES

- [1] D. Shah, B. Yang, S. Kriegman, M. Levin, J. Bongard, and R. Kramer-Bottiglio, "Shape changing robots: Bioinspiration, simulation, and physical realization," *Advanced Materials*, p. 2002882, 2020.
- [2] E. D. Demaine, M. L. Demaine, and V. Hart, "Computational balloon twisting: The theory of balloon polyhedra," in *CCCG*, 2008.
- [3] N. S. Usevitch, Z. M. Hammond, M. Schwager, A. M. Okamura, E. W. Hawkes, and S. Follmer, "An untethered isoperimetric soft robot," *Science Robotics*, vol. 5, no. 40, 2020.
- [4] R. Comer and S. Levy, "Deflections of an inflated circular-cylindrical cantilever beam," *AIAA journal*, vol. 1, no. 7, pp. 1652–1655, 1963.
- [5] W. Fichter, *A theory for inflated thin-wall cylindrical beams*. National Aeronautics and Space Administration, 1966.
- [6] M. Yim, W.-M. Shen, B. Salemi, D. Rus, M. Moll, H. Lipson, E. Klavins, and G. S. Chirikjian, "Modular self-reconfigurable robot systems [grand challenges of robotics]," *IEEE Robotics & Automation Magazine*, vol. 14, no. 1, pp. 43–52, 2007.
- [7] J. Seo, J. Paik, and M. Yim, "Modular reconfigurable robotics," *Annual Review of Control, Robotics, and Autonomous Systems*, vol. 2, pp. 63–88, 2019.
- [8] Y. Kim and M. A. Minor, "Distributed kinematic motion control of multi-robot coordination subject to physical constraints," *The International Journal of Robotics Research*, vol. 29, no. 1, p. 92–109, 2009.
- [9] Y. Kim and M. Minor, "Coordinated kinematic control of compliantly coupled multirobot systems in an array format," *IEEE Transactions on Robotics*, vol. 26, no. 1, p. 173–180, 2010.
- [10] D. Rus and M. T. Tolley, "Design, fabrication and control of soft robots," *Nature*, vol. 521, no. 7553, pp. 467–475, 2015.
- [11] C. Majidi, "Soft robotics: a perspective—current trends and prospects for the future," *Soft Robotics*, vol. 1, no. 1, pp. 5–11, 2014.
- [12] E. W. Hawkes, L. H. Blumenschein, J. D. Greer, and A. M. Okamura, "A soft robot that navigates its environment through growth," *Science Robotics*, vol. 2, no. 8, p. eaan3028, 2017.
- [13] M. Takeichi, K. Suzumori, G. Endo, and H. Naba, "Development of a 20-m-long giacometti arm with balloon body based on kinematic model with air resistance," in *2017 IEEE/RSJ International Conference on Intelligent Robots and Systems (IROS)*. IEEE, 2017, pp. 2710–2716.
- [14] Z. M. Hammond, N. S. Usevitch, E. W. Hawkes, and S. Follmer, "Pneumatic reel actuator: Design, modeling, and implementation," in *Robotics and Automation (ICRA), 2017 IEEE International Conference on*. IEEE, 2017, pp. 626–633.
- [15] N. S. Usevitch, A. M. Okamura, and E. W. Hawkes, "Apam: antagonistic pneumatic artificial muscle," in *2018 IEEE International Conference on Robotics and Automation (ICRA)*. IEEE, 2018, pp. 1539–1546.
- [16] S. Voisembert, A. Riwan, N. Mechbal, and A. Barraco, "A novel inflatable robot with constant and continuous volume," in *2011 IEEE International Conference on Robotics and Automation*. IEEE, 2011, pp. 5843–5848.
- [17] B. H. Do, V. Banashek, and A. M. Okamura, "Dynamically reconfigurable discrete distributed stiffness for inflated beam robots," in *2020 IEEE International Conference on Robotics and Automation (ICRA)*, 2020, pp. 9050–9056.
- [18] M. T. Gillespie, C. M. Best, and M. D. Killpack, "Simultaneous position and stiffness control for an inflatable soft robot," *2016 IEEE International Conference on Robotics and Automation (ICRA)*, 2016.
- [19] M. Jiang, Q. Yu, and N. Gravish, "Vacuum induced tube pinching enables reconfigurable flexure joints with controllable bend axis and stiffness," *2021 IEEE 4th International Conference on Soft Robotics (RoboSoft)*, 2021.
- [20] J. M. M. Tur and S. H. Juan, "Tensegrity frameworks: Dynamic analysis review and open problems," *Mechanism and Machine Theory*, vol. 44, no. 1, pp. 1–18, 2009.
- [21] K. Kim, L.-H. Chen, B. Cera, M. Daly, E. Zhu, J. Despois, A. K. Agogino, V. SunSpiral, and A. M. Agogino, "Hopping and rolling locomotion with spherical tensegrity robots," *2016 IEEE/RSJ International Conference on Intelligent Robots and Systems (IROS)*, 2016.
- [22] A. P. Sabelhaus, J. Bruce, K. Caluwaerts, P. Manovi, R. F. Firoozzi, S. Dobi, A. M. Agogino, and V. SunSpiral, "System design and locomotion of superball, an untethered tensegrity robot," *2015 IEEE International Conference on Robotics and Automation (ICRA)*, 2015.
- [23] M. Vespignani, J. M. Friesen, V. SunSpiral, and J. Bruce, "Design of superball v2, a compliant tensegrity robot for absorbing large impacts," *2018 IEEE/RSJ International Conference on Intelligent Robots and Systems (IROS)*, 2018.
- [24] G. J. Hamlin and A. C. Sanderson, "Tetrobot modular robotics: Prototype and experiments," in *Intelligent Robots and Systems '96, IROS 96, Proceedings of the 1996 IEEE/RSJ International Conference on*, vol. 2. IEEE, 1996, pp. 390–395.
- [25] S. Curtis, M. Brandt, G. Bowers, G. Brown, C. Cheung, C. Cooperider, M. Desch, N. Desch, J. Dorband, K. Gregory *et al.*, "Tetrahedral robotics for space exploration," *IEEE Aerospace and Electronic Systems Magazine*, vol. 22, no. 6, pp. 22–30, 2007.
- [26] A. Lyder, R. F. M. Garcia, and K. Stoy, "Mechanical design of odin, an extendable heterogeneous deformable modular robot," in *Intelligent Robots and Systems, 2008. IROS 2008. IEEE/RSJ International Conference on*. IEEE, 2008, pp. 883–888.
- [27] C.-H. Yu, K. Haller, D. Ingber, and R. Nagpal, "Morpho: A self-deformable modular robot inspired by cellular structure," in *2008 IEEE/RSJ International Conference on Intelligent Robots and Systems*. IEEE, 2008, pp. 3571–3578.
- [28] J. C. Zagal, C. Armstrong, and S. Li, "Deformable octahedron burrowing robot," in *Artificial Life Conference Proceedings 12*. MIT Press, 2012, pp. 431–438.
- [29] A. Spinos, D. Carroll, T. Kientz, and M. Yim, "Variable topology truss: Design and analysis," in *2017 IEEE/RSJ International Conference on Intelligent Robots and Systems (IROS)*. IEEE, 2017, pp. 2717–2722.
- [30] M. Pieber, R. Neurauder, and J. Gerstmayr, "An adaptive robot for building in-plane programmable structures," in *2018 IEEE/RSJ International Conference on Intelligent Robots and Systems (IROS)*. IEEE, 2018, pp. 1–9.
- [31] D. Vella, H. Ebrahimi, A. Vaziri, and B. Davidovitch, "Wrinkling reveals a new isometry of pressurized elastic shells," *EPL (Europhysics Letters)*, vol. 112, no. 2, p. 24007, 2015.
- [32] N. S. Usevitch, Z. M. Hammond, and M. Schwager, "Locomotion of linear actuator robots through kinematic planning and nonlinear optimization," *IEEE Transactions on Robotics*, 2020.
- [33] C. Liu, S. Yu, and M. Yim, "A fast configuration space algorithm for variable topology truss modular robots," in *2020 IEEE International Conference on Robotics and Automation (ICRA)*. IEEE, 2020, pp. 8260–8266.
- [34] C. Liu and M. Yim, "Reconfiguration motion planning for variable topology truss," in *2019 IEEE/RSJ International Conference on Intelligent Robots and Systems (IROS)*. IEEE, 2019, pp. 1941–1948.